https://doi.org/10.5194/wes-2022-36
Preprint. Discussion started: 8 April 2022

Wind tunnel investigation of the aerodynamic response of two 15 MW floating wind turbines

Alessandro Fontanella[1], Alan Facchinetti[1], Simone Di Carlo[1], and Marco Belloli[1]

[1]Mechanical Engineering Department, Politecnico di Milano, Milano, Via La Masa 1, 20156, Italy.

Correspondence: Alessandro Fontanella (alessandro.fontanella@polimi.it)

Abstract. The aerodynamics of floating turbines is complicated by large motions which are permitted by the floating foundation, and the interaction between turbine, wind and wake is not yet fully understood. The object of this paper is a wind tunnel campaign finalized at characterizing the aerodynamic response of a 1:100 scale model of the IEA 15 MW subjected to imposed platform motion. The turbine aerodynamic response is studied focusing on thrust force, torque and wake at 2.3D downwind the rotor. Harmonic motion is imposed in the surge, sway, roll, pitch and yaw directions with several frequencies and amplitudes, which are selected to be representative of the two 15 MW floating turbines developed within the COREWIND project. Thrust and torque show large-amplitude oscillations with surge and pitch motion, which main effect is an apparent wind speed; oscillations in thrust and torque are negligible with the other motions, which main effect is to alter the wind direction. The thrust and torque response measured in the experiment is compared with predictions of a quasi-steady model, often used for control-related tasks. The agreement is good in case of low-frequency surge motion, but some differences are seen in the pitch case. The quasi-steady model is not predictive for the response to wave-frequency motion, where blade unsteadiness may take place. Wake was measured imposing motion in five directions with frequency equal to the wave-peak frequency. The axial speed is slightly lower with motion compared to the fixed case. The turbulence kinetic energy is slightly lower too. Wave-frequency motion seems to produce a more stable and lower flow mixing.

1 Introduction

Floating offshore wind turbines (FOWTs) have numerous advantages over their bottom-fixed counterpart when it comes to harnessing the wind power resource of deep-sea sites, which make up a significant portion of the offshore wind resource. Wind speed is generally higher in these regions which are further from the coast, but bottom-fixed foundations are not cost effective when the water depth is higher than 50 m, and installation could be easier as most operations can be done in a port. Technical feasibility has been proved by a first wave of pre-commercial projects deployed worldwide, and the second phase of offshore floating wind power is underway with the first pilot floating farms being developed in these years (Barter et al. (2020)). Installed floating wind power is expected to grow significantly over the next few years, but there are still many technical challenges to be solved to make this possible. Floating wind has been included by Veers et al. (2019) among the open research questions in the science of wind energy. The large dimensions of modern machines combined with the additional degrees of freedom of floating foundations give rise to new interactions between the turbine, the wind and wakes, which are not yet fully understood. Most

https://doi.org/10.5194/wes-2022-36
Preprint. Discussion started: 8 April 2022

studies about the design and response of floating wind turbines implicitly assume the aerodynamic analysis methods developed for bottom-fixed turbines are valid also in the floating case (Sebastian and Lackner (2013)), so data is needed to evaluate the capabilities of such models.

In this sense, scale model experiments which focus is the aerodynamic response in floating turbines, like the one covered in this article, are useful in two ways: to gain knowledge about the physics of the process, and for producing datasets for codes validation. Farrugia et al. (2014) carried out experiments with the scale model of a TLP turbine subjected to different wave and turbine operating conditions, and analyzed the effect of wave-induced motions on the turbine power output and wake comparing results for the floating case to the bottom-fixed condition. With the support of a free vortex wake code, it is shown that platform motion causes fluctuations in the aerodynamic torque, a reduced mean power coefficient, and a time-varying tip-vortex transport velocity. Rockel et al. (2014) measured the wake of a model wind turbine with PIV with platform pitch motion and compared it with four wake models. The wake structure has been found to be more complex with rigid-body motions and this requires developing improved wake models. Fu et al. (2019) conducted wind tunnel experiments to understand the effect of platform pitch and roll motion on the power output and wake of a model turbine. It is shown the wake is significantly altered by imposed motion, and the power fluctuations exhibit a marked peak in the spectral content in correspondence of the frequency of motion. Bayati et al. (2016) conducted a wind tunnel campaign with a scale model of the DTU 10MW subjected to imposed surge and pitch motion and compared thrust measurements to a BEM model with dynamic wake. This experiment was complemented by a second (Bayati et al. (2017b)) focused on the effects of imposed surge motion on the wake. It is seen the wake axial velocity has fluctuations at the frequency of motion and the amplitude of these oscillations depends on the average thrust coefficient, and the frequency of motion. The findings of these two experiments, and the lack of clear conclusions, promoted the UNsteady Aerodynamics of FLOating Wind turbines (UNAFLOW) project which goal was to study the aerodynamic response of an FOWT subjected to large surge motion, covering blade forces, rotor-integral forces, and wake. The methodology and experimental results of the experiment are discussed in the articles of Bayati et al. (2018a), Bayati et al. (2018b), and Fontanella et al. (2021a). Among the project results, it is found the turbine thrust response is quasi-static for reduced frequency up to 0.5, the near-wake energy content is increased in correspondence of the frequency of motion, and the travel speed of the tip-vortex has periodic oscillations. Schliffke et al. (2020) studied the wake of an FOWT with imposed surged motion by means of a porous-disk model placed in an atmospheric boundary layer wind tunnel. Results show the turbulence intensity in the far-wake is lower for a floating turbine compared to the bottom-fixed case, and the spectral content of the axial velocity has a peak at the frequency of imposed motion.

As said, experimental data are useful for validation of aerodynamic codes. The dataset of the UNAFLOW experiment is currently examined in the Phase III of the OC6 project, where experimental data are compared to numerical tools which are based on different principles and have a variable fidelity level. Previous efforts are the work of Cormier et al. (2018), which used the UNAFLOW data to assess predictions of a BEM model, a free vortex wake model, and a blade-resolved computational fluid dynamics (CFD) model, and of Mancini et al. (2020) which focused on rotor forces and extended the comparison to an actuator line model.

https://doi.org/10.5194/wes-2022-36
Preprint. Discussion started: 8 April 2022

The research in this work investigates the aerodynamic response of two 15 MW floating turbines developed in the COREWIND project (Mahfouz et al. (2021)). An experimental testing campaign has been conducted at the Politecnico di Milano wind tunnel with a 1:100 model of the IEA 15 MW turbine which was subjected to imposed platform motion so to simulate the rigid-body movement of a floating turbine. The main contributions of this work are as follows.

- Previous experiments have shown that platform motion affects the turbine aerodynamic response, primarily the thrust force, the rotor torque (and power) and the turbine wake, but conclusions are still partial. In this sense, we decided to investigate the above mentioned quantities, but, differently than in previous experiments, we analyzed the turbine response to motion in all directions. The imposed motion is sinusoidal and in one direction at a time, so it is still idealized, but the test matrix is defined to be representative of the motion of a 15 MW floating turbine in a realistic deployment site. To this end we considered the Activefloat and WindCrete floating turbines developed in the COREWIND project with reference to the Gran Canaria site (Mahfouz et al. (2021)). The sinusoidal motion was preferred over a more realistic one, with the platform moving simultaneously in all directions and in a broad frequency range, to ease future comparisons with numerical codes. Past test campaigns at Politecnico di Milano focused on the response to low-frequency motion where the movement of the system is large because of resonant excitation. Large motion is also expected in the wave frequency range, which is addressed in the present campaign.
- The aerodynamic thrust and torque is often introduced in control-oriented models of floating turbines by means of the static power and thrust coefficients and, when the model is linearized, by means of their gradient with respect to blade pitch, rotor speed and wind speed. Here, we try to assess if and when the modeling approach based on the static power and thrust coefficients is effective, comparing its predictions with the thrust and torque response to surge and pitch motion.
- The wind tunnel measurements of Bayati et al. (2018a), Bayati et al. (2018b), and Fontanella et al. (2021a) focused on the wake-flow response with low-frequency surge motion. In this campaign wake was measured with motion in five directions with a typical wave frequency. Wake is measured in non-turbulent inflow conditions to highlight the effect of turbulence produced by the floater motion on the flow mixing and wake recovery.

The foreseen impact of this paper is as follows.

- The database of force measurements can be used for validation of numerical codes. Recent validation tasks focused on the force response to low-frequency surge and pitch motion. With data of this campaign, the comparison can be extended to higher frequencies and to other directions of motion. Moreover, one goal of the COREWIND project is to use a combination of hybrid hardware-in-the-loop experiments in the wind tunnel (Belloli et al. (2020)) and in the wave basin (Battistella et al. (2018)) for assessing the response of two 15 MW floating turbines in operating and extreme conditions. In wave basin hybrid experiments aerodynamic loads are simulated with a force actuator and an aerodynamic model of the turbine. Wind tunnel measurements of the force response can be used for tuning this model. Having calibrated the aerodynamic part of the wave basin experiment on the response of the turbine model should favor the comparison of hybrid wave basin results with results of hybrid wind tunnel experiments that use the same turbine model.

- Comparison of wind tunnel results with the control-oriented model of the thrust and torque response to turbine motion gives an idea of where this is valid and where it may have some shortfalls.
- With the recent progress of the floating turbine technology, studies are emerging about the response and control of floating wind farms, like the one about loads and wake meandering of Wise and Bachynski (2020) and the one about vertical wake steering of Nanos et al. (2021). Wind tunnel measurements of the wake inflow increase knowledge about wakes of floating turbines, and this is of utmost importance for pushing further the floating wind technology.

The structure of the remainder of this paper is as follows. Section 2 describes the testing facility, the turbine scale model and the measurements that were carried out. The load cases of the experiment, and the rationale behind their definition, are discussed in Sect. 3. Section 4 presents the results about rotor forces with fixed and moving turbine, and here experimental results with surge and pitch motion are compared to quasi-static linear model. Results about the turbine wake with different types of platform motion are reported in Sect. 5. Graphs of the results section are made in accordance with the recommendations of Stoelzle and Stein (2021) to improve data perception. Finally, Sect. 6 discusses some conclusions and tries to give some suggestions for future work about the aerodynamic response of floating turbines.

2 Experimental campaign

The testing activity was carried out in the atmospheric boundary layer test section of the Politecnico di Milano wind tunnel (GVPM), which has dimensions: 13.84 m wide x 3.84 m high x 35 m long. The test setup is shown in Fig. 1. The turbine was mounted on a 6-DOFs robotic platform to enable forced motion.

2.1 Scale turbine design and specifications

The wind turbine is a 1:100 scale model of the IEA 15 MW (Allen et al. (2020)). The turbine rotor was scaled to preserve the power (C_P) and thrust (C_T) coefficients of the reference turbine despite the reduced size and a wind speed reduction factor of 3. The blade design is carried out to match the lift distribution along the span while preserving the tip-speed ratio, similarly to what was done by Bayati et al. (2017a) for a 1:75 model of the DTU 10 MW. The blade chord is increased with respect to the reference full-scale rotor preserving the original distribution, the twist distribution is altered to have the target non-dimensional lift force. The turbine tower, of 75 mm diameter, is rigid since we focus on the effect of rotor motion associated with platform motion rather than with tower deformability. The turbine has individual blade-pitch control and variable-speed generator control. The blades were built to be rigid to exclude any aeroelastic interaction, which was outside of the scope of this research. The main properties of the turbine model are summarized in Table 1.

https://doi.org/10.5194/wes-2022-36
Preprint. Discussion started: 8 April 2022

Open Access
WIND ENERGY SCIENCE DISCUSSIONS

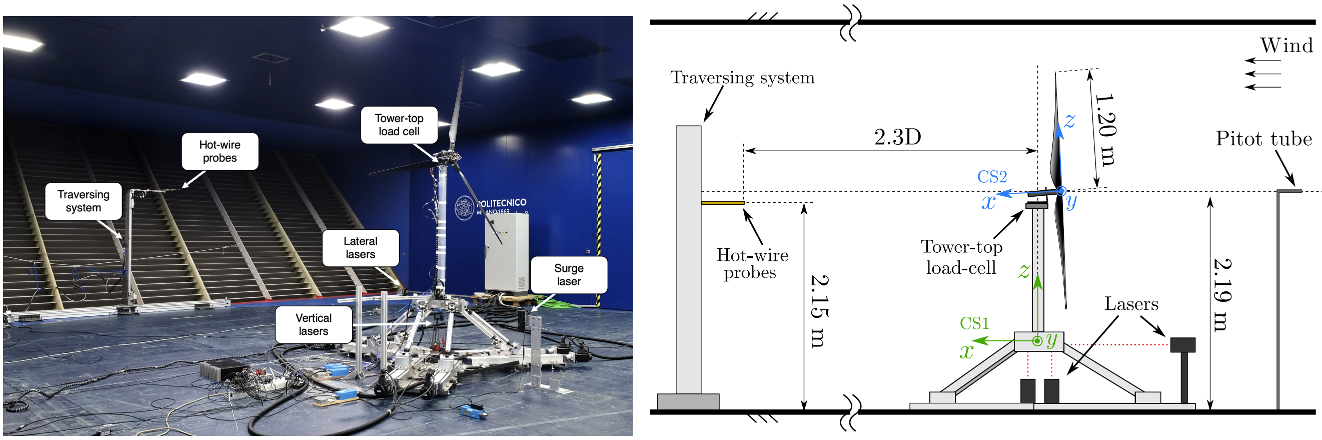

Figure 1. Experimental setup in the Polimi wind tunnel (left) and schematic of the test setup with the coordinate systems (CS) used for measurements and their analysis (right).

Table 1. Key parameters of the wind turbine model.

Parameter	Unit	Value
Rotor diameter	m	2.400
Blade length	m	1.110
Hub diameter	m	0.180
Rotor overhang	m	0.139
Tilt angle	°	5.000
Tower-to-shaft	m	0.064
Tower diameter	m	0.075
Tower length	m	1.400
Nacelle mass	kg	1.975
Blade mass	kg	0.240
Rotor mass	kg	2.041
Tower mass	kg	2.190

2.2 Measurements

The measurements taken in the tests are shown in Fig. 1 and are: interface forces between tower-top and nacelle by a 6-components load cell; platform position by laser transducers; 3-components (u, v, and w) wind velocity in the wake by hot-wire probes. The two probes were moved in the cross-wind direction (Y) of CS1, from -1.6 m to $+1.6$ m with a discretization of 100 mm, at a fixed distance X = 2.3D, and Z = 2.15 m. The undisturbed wind velocity was measured by a pitot tube 7.15 m

https://doi.org/10.5194/wes-2022-36
Preprint. Discussion started: 8 April 2022

upstream of the turbine rotor, centerline, and hub height (not visible in the picture of Fig. 1). All measurements were sampled synchronously at 2 kHz and stored at model scale.

3 Definition of load cases

The experiment considered two wind turbine functioning conditions reported in Table 2: one is representative of below rated wind operations, where rotor speed is controlled to achieve the maximum power coefficient; and one for above rated wind, where the blade pitch angle is adjusted to regulate power at its rated value. Active turbine control was not used, and in all tests the blade pitch angle and rotor speed were constant. All tests were performed using an empty inlet configuration (i.e., without roughness elements or turbulence generators) for a uniform inflow velocity and a resulting turbulence intensity around 2%.

Table 2. Wind turbine operating conditions considered in the experiment (CP is collective pitch).

Condition	Wind speed [m/s]	Rotor speed [RPM]	TSR [-]	CP [°]
Below rated (BR)	3.0	210	8.8	-3.5
Above rated (AR)	5.0	216	5.4	8.5

For the cases with motion, the turbine was forced to oscillate alternatively in the surge, sway, roll, pitch, and yaw degree-of-freedom (DOF). As it is noticed by Sebastian and Lackner (2013), the platform motions modify the operating environment for the turbine rotor compared to the bottom fixed case, mostly by altering the apparent wind speed perceived by the rotor disk. Different movements have a different effects:

- surge, pitch, and yaw move the rotor disk in the wind direction altering the magnitude of wind speed. In the surge case, the additional wind speed due to motion is constant across the rotor, in the pitch case it increases linearly with height, with yaw the increment is linear with radial distance and of opposite sign on the left and right side of the rotor;
- pitch, roll, and yaw introduce an effective wind shear;
- sway, heave, and roll move the rotor in the cross-wind direction and modify the angle formed by wind with the rotor axis, creating a skewed (i.e., non-axial) inflow.

When the wind is constant and uniform in space, the effect of sway and heave in terms of apparent wind perceived by rotor is similar: one inclines the velocity vector in the horizontal plane, and the other in the vertical plane. At the same time, the wind tunnel section is large compared to rotor ($A_{\mathrm{rotor}}/A_{\mathrm{tunnel}}$ = 0.08) but its height is comparable to the rotor diameter (D/h_{tunnel} = 0.62) and this is cause of anisotropic blockage. In reason of these two considerations, the turbine was moved only in the sway direction.

https://doi.org/10.5194/wes-2022-36
Preprint. Discussion started: 8 April 2022

The motion for every DOF was imposed at three frequencies: the natural frequency of the mode for the Activefloat and for the WindCrete, and the frequency of the wave spectrum peak for the deployment site of Gran Canaria as reported by Mahfouz et al. (2021) (i.e., 0.11 Hz corresponding to 3.175 Hz at model scale). Reduced frequency is a dimensionless number used to characterize the degree of unsteadiness of an aerodynamic system which is caused by a harmonic perturbation in the flow. The rotor reduced-frequency f_r is used for describing the rotor-level unsteadiness, associated with the global response of the rotor disk and its wake. It is defined as:

$$f_r = \frac{f_m \mathrm{D}}{U_\infty}, \tag{1}$$

where f_m is the frequency of motion, U_∞ the free-stream wind speed, and D the diameter of the turbine rotor. The reduced frequency of the load cases of the experiment is shown in Fig. 2. Results of the testing of Fontanella et al. (2021a) indicate surge motion causes minimal unsteady aerodynamic behavior when f_r is lower than 0.5. In the experiment discussed in this paper f_r was increased up to 3 to verify if the conclusions of Fontanella et al. (2021a) are valid for motion at the wave frequency. Results of different studies about the aerodynamic wind turbines are presented as function of f_r in the article of Ferreira et al. (2021).

At the same time, blade-level unsteadiness may occur, as predicted for example by Theodorsen theory, when the blade reduced-frequency f_c is larger than 0.5. Beyond this threshold, the apparent mass effects due to local flow acceleration become dominant, and the airfoil aerodynamic behavior is no more quasi-steady. The blade reduced-frequency f_c is defined as:

$$f_c = \frac{f_m c}{2U_\infty}, \tag{2}$$

where $c/2$ is the blade semi-chord. As done by Sebastian and Lackner (2013), it is possible to define a threshold frequency for turbine motion beyond which airfoil-level unsteadiness may occur:

$$f_{m,th} = \frac{0.05\sqrt{U_\infty^2 + (r\omega_r)^2}}{\pi c}, \tag{3}$$

where ω_r is the rotor speed and r the radial position of a blade section. The threshold frequency for the turbine scale model and the two operating conditions of the experiment is reported in Fig. 2. The shaded area in the figure corresponds to the operating range of the IEA 15 MW. Motion with frequency that falls to the right of the curve may cause blade-level unsteadiness. The blade aerodynamic response is quasi-steady for motion at the natural frequencies of the two floating turbines. Motion with frequency of the WindCrete yaw mode and at the wave frequency may result in some unsteadiness for the blade section with $r/R < 0.5$. For the last two conditions, blade-level and rotor-level unsteady aerodynamics may occur together, whereas only rotor-level unsteadiness is expected at the other motion frequencies.

Equations 1-2 account for the motion frequency, but not its amplitude. When the motion frequency is high, the rotor or blade aerodynamics may be different than the quasi-steady prediction, but the effects of unsteadiness may be small if the motion amplitude is small.

In this experiment the three frequencies f_m where tested with two values of amplitude for any platform DOF to assess the dependence of the system behavior on the motion amplitude. The motion amplitudes A_m were defined with the following rules:

https://doi.org/10.5194/wes-2022-36
Preprint. Discussion started: 8 April 2022

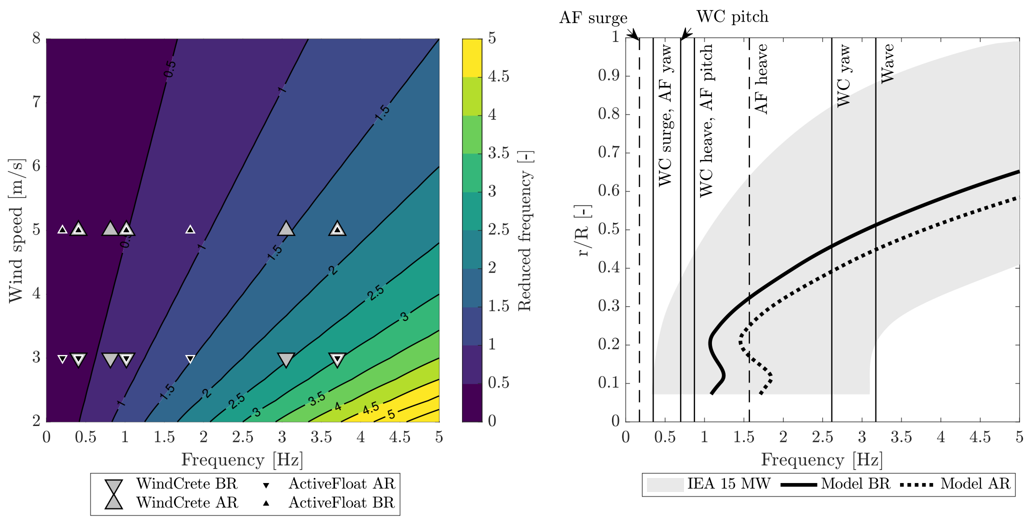

Figure 2. Left: rotor reduced-frequency as a function of motion frequency and wind speed; the reduced frequencies of the load cases are identified by markers (BR is below rated, AR above rated). Right: the threshold motion frequency beyond which blade-level unsteady aerodynamics may occur for the turbine model is compared to the motion frequencies of the experiments (AF is Activefloat, WC is WindCrete); the shaded area covers the threshold frequency for the IEA 15 MW in its operating range.

- surge: to produce a normalized maximum velocity $\Delta u/U_\infty$ = 0.04-0.05, where $\Delta u = 2\pi f_m A_m$. The resulting amplitude values are between 0.010 m and 0.180 m (1.0-18.0 m full-scale). The values of $\Delta u/U_\infty$ are chosen to be similar to those used in the campaign of Fontanella et al. (2021a) to facilitate comparison with the results of that test.
- pitch: to have a normalized maximum velocity at hub height $\Delta u_{\mathrm{hh}}/U_\infty$ = 0.04-0.05, where $\Delta u_{\mathrm{hh}} = 2\pi f_m A_m d_{\mathrm{hub}}$, and d_{hub} the distance between the rotor apex and the center of pitch rotation. With this choice, the apparent wind speed at the hub due to motion is the same of surge cases. The main effect of surge and pitch motion is to alter the wind speed perceived by the rotor, so having the same ΔU_{hh} should favor comparisons between the surge and pitch load cases. The pitch motion is between 0.25-2.76 deg;
- yaw: to give a normalized maximum velocity of the rotor edge $\Delta u_R/U_\infty$ = 0.03, 0.05, with $\Delta u_R = 2\pi f_m A_m R$. In this way, the wind speed perceived by the outermost sections of the blade is similar to surge cases. The resulting yaw motion has amplitude of 0.3-3.0 deg;
- sway: to give a maximum wind misalignment with respect to rotor axis $\alpha = 2°, 4°$, where $\alpha = \tan^{-1}(2\pi f_m A_m/U_\infty)$. The amplitude of motion is in the range 0.011-0.064 m (1.1-6.4 m full-scale);
- roll: to have a maximum wind misalignment at hub height $\alpha_{\mathrm{hh}} = 2°, 4°$, where $\alpha = \tan^{-1}(2\pi f_m A_m z_{\mathrm{hh}}/U_\infty)$, and z_{hh} is the vertical distance between rotor apex and the roll axis. The wind misalignment is the same of sway cases, and the amplitude of motion is of 0.4-3.0 deg.

https://doi.org/10.5194/wes-2022-36
Preprint. Discussion started: 8 April 2022

eawe european academy of wind energy
Open Access WIND ENERGY SCIENCE DISCUSSIONS

The complete test matrix obtained with the rules above is reported in Appendix A. The lowest values of the motion amplitude are representative of 15 MW floating turbines in operational conditions (OpenFast simulations about the Activefloat and Wind-Crete floating turbines are presented by Mahfouz et al. (2021)), the highest values are instead useful to assess the aerodynamic response in a limit case. Wake measurements are carried out for motion conditions with f_m = 3.175 Hz.

4 Results about rotor forces

The global response of a FOWT is influenced by rotor-integral loads which are often identified in the combined thrust force and torque of the three blades (e.g., by Lemmer et al. (2020a)). The torque is strictly connected to the turbine power output, the dynamics of the drivetrain and the controller response. In a wind turbine, power is extracted from wind at the expense of a thrust force exerted on the rotor, which results in the rigid and flexible motion of the structure in the along-wind direction (van der Veen et al. (2012)). Thrust and torque are state-dependent because the motion of the structure produces an apparent wind which affects the rotor loads. Hereafter, we report and discuss the experimental results in terms of these rotor forces.

The thrust force and torque, expressed in the CS2 reference frame which is non-rotating and fixed to the rotor hub, are obtained projecting the force measurements of the tower-top load cell. Results for the fixed turbine are reported in terms of steady-state power and thrust coefficients. Results for the fixed turbine are the filtered time series of the torque and thrust oscillations with different types of motion. The thrust/torque response with surge and pitch is compared to a linear quasi-steady model, which is often used for control purposes.

4.1 Fixed turbine

The power and thrust coefficient of the turbine scale model with steady wind and no motion are compared to those of the IEA 15 MW in Table 3. The scaled rotor performs close to the full-scale turbine. The thrust coefficient, which primarily depends on the distribution of normal force along the blade, is closely matched. As discussed by Wang et al. (2021), the axial velocity in the wake is largely set by the rotor thrust, and the wake of the turbine scale model is representative of the full-scale turbine if the thrust coefficient is the same. Some mismatch is instead seen for the power coefficient. This is largely influence by airfoil efficiency, which is lower for the turbine scale model.

Table 3. Steady power (C_P) and thrust (C_T) coefficient for the wind turbine model (subscript "WTM") and for the IEA 15 MW (subscript "ref") in the operating conditions of the experiment (see Table 2).

Condition	$C_{P,\mathrm{WTM}}$ [-]	$C_{P,\mathrm{ref}}$ [-]	$C_{T,\mathrm{WTM}}$ [-]	$C_{T,\mathrm{ref}}$ [-]
Below rated (BR)	0.35	0.49	0.78	0.77
Above rated (AR)	0.13	0.17	0.20	0.20

https://doi.org/10.5194/wes-2022-36
Preprint. Discussion started: 8 April 2022

In addition, the blade pitch-TSR maps of the power and thrust coefficient were measured in steady wind with U_∞ = 4 m/s, with a resolution for TSR of 0.3 and 3° for blade pitch. The maps are reported in Fig. 3.

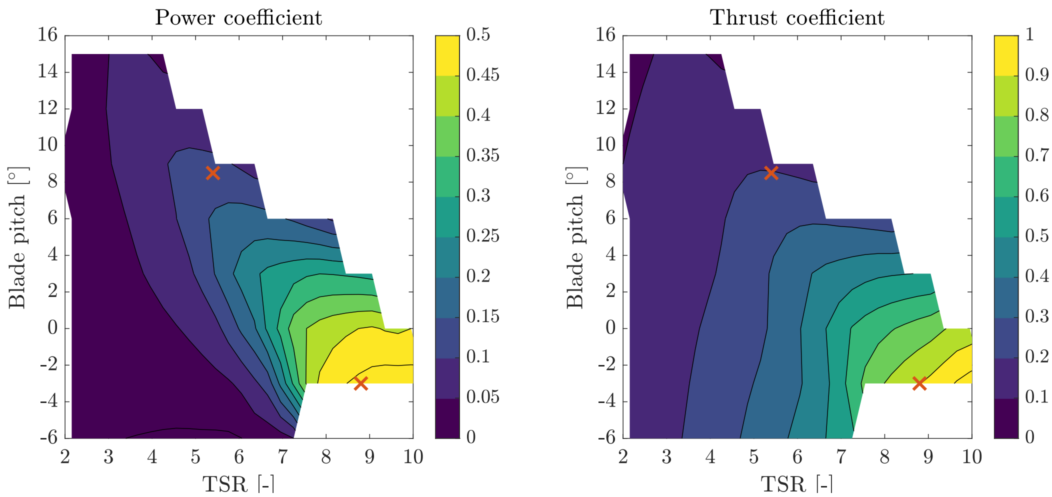

Figure 3. Map of the power and thrust coefficients of the turbine model measured in steady wind with U_∞ = 4 m/s. The × marks correspond to the operating conditions of Table 3.

4.2 Moving turbine

Force measurements with moving turbine are processed as depicted in Fig. 4 in order to remove the contribution of the rotor-nacelle inertia associated with the motion of the structure. For every load case two tests are run imposing the same motion to the turbine base: one with no wind and fixed rotor, and one with wind and spinning rotor. Measurements of the two tests are windowed so to have the same integer number of periods of the imposed motion. Time series of the 6 tower-top forces from the no-wind tests are subtracted from the time series of the test with wind. In doing this operation, we assume the flexible response of the turbine is small (i.e., the model is rigid) and equal with and without wind; we also assume the aerodynamic force developed by the blades is small in the test without wind. The forces obtained with the force subtraction procedure are projected to CS2. The focus of the analysis is the thrust/torque response at the frequency of platform motion. Hence, we compute the FFT and we alternatively look at the amplitude and phase of the harmonic component with frequency equal to the frequency of motion, or its IFFT. In the figures below time series obtained from the IFFT are labelled as “Filtered”.

The harmonic components of thrust and torque at the frequency of imposed motion, in all the wind and motion conditions we studied are reported in Fig. 5. For thrust, the oscillations with the largest amplitude are observed with surge and pitch motion. For motion of equal frequency and the same normalized variation of wind speed, the amplitude of oscillations is larger in above rated than in below rated: the amplitude of thrust oscillations depends on the operating condition. With the other motions, oscillations are small and of the same order of magnitude of the response to the inflow turbulence. Motions in directions other than the wind direction do not affect the turbine thrust in a significant way. Torque oscillations are of

https://doi.org/10.5194/wes-2022-36
Preprint. Discussion started: 8 April 2022

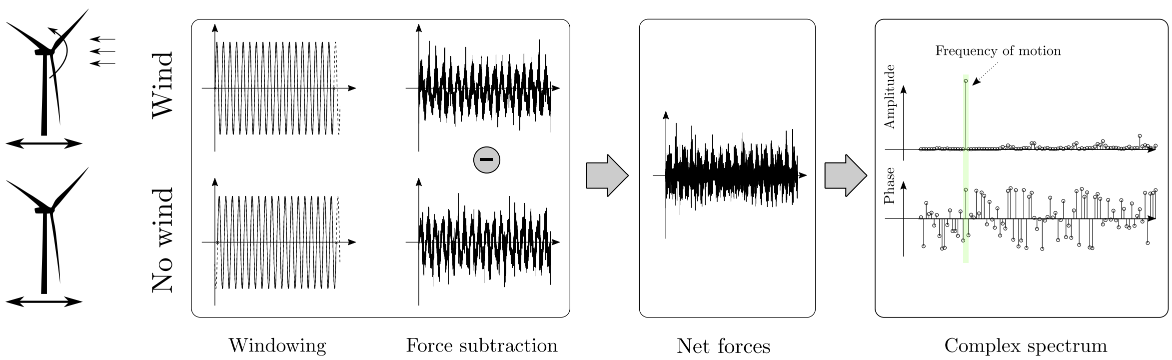

Figure 4. Scheme of the post-processing applied to force measurements in tests with moving turbine. Two tests are carried out for every motion condition, one with wind and spinning rotor, one without wind and with still rotor. Time series from the two tests are windowed so to have the same integer number of motion periods. Then, forces from the test with no wind are subtracted from forces with wind. The resulting forces are examined taking the complex spectrum and studying the harmonic content at the frequency of the imposed motion.

meaningful amplitude with surge, pitch, sway and roll. For surge cases with $f_m < 3.175$ Hz (the corresponding rotor-reduced frequency is 2.5 in below-rated wind and 1.5 in above-rated wind), the peak of thrust and torque is when the motion phase is equal to π, which corresponds to the turbine moving upwind and passing from the rest position, and the wind speed experienced by the rotor is the maximum during the motion cycle. With $f_m = 3.175$, the peak is delayed. As shown in Fig. 2, motion with $f_m = 3.175$ is associated with blade-level unsteadiness for sections with $r/R < 0.5$ and this unsteadiness, absent at the other frequencies of surge motion, may explain the larger phase shift. The peak-to-peak amplitude with pitch is similar to the one with surge motion for equal amplitude of hub displacement; it is more difficult to see a trend in the phase shift, which is not π. Large torque oscillations are also seen with roll and sway. The amplitude is proportional to the frequency of motion and the peak is shifted of $\pm\pi/2$ with respect to motion; the maximum is when the acceleration due to platform motion is directed as the blade peripheral speed. In this respect, it is worth remembering the force post-processing removes the inertial component of force measurements with blades in a given azimuth position (the one of the test without wind), but leaves out the additional inertial torque due to side acceleration with spinning rotor.

4.2.1 Quasi-static model of thrust and torque

The thrust and torque response to surge and pitch is compared with the prediction of a linear quasi-static model, which is often used when dealing with control of floating turbines. The surge and pitch DOFs are usually included in control-oriented models (e.g., those of van der Veen et al. (2012), Pegalajar-Jurado et al. (2018), Fontanella et al. (2020), Lemmer et al. (2020a)) because these show the largest response amplitude among all the platform motions when wind and waves are aligned. Generally, in such models the aerodynamic rotor thrust is introduced as

$$F_x = \frac{1}{2}\rho C_T(\omega_r,\beta,U)A_rU^2, \tag{4}$$

https://doi.org/10.5194/wes-2022-36
Preprint. Discussion started: 8 April 2022

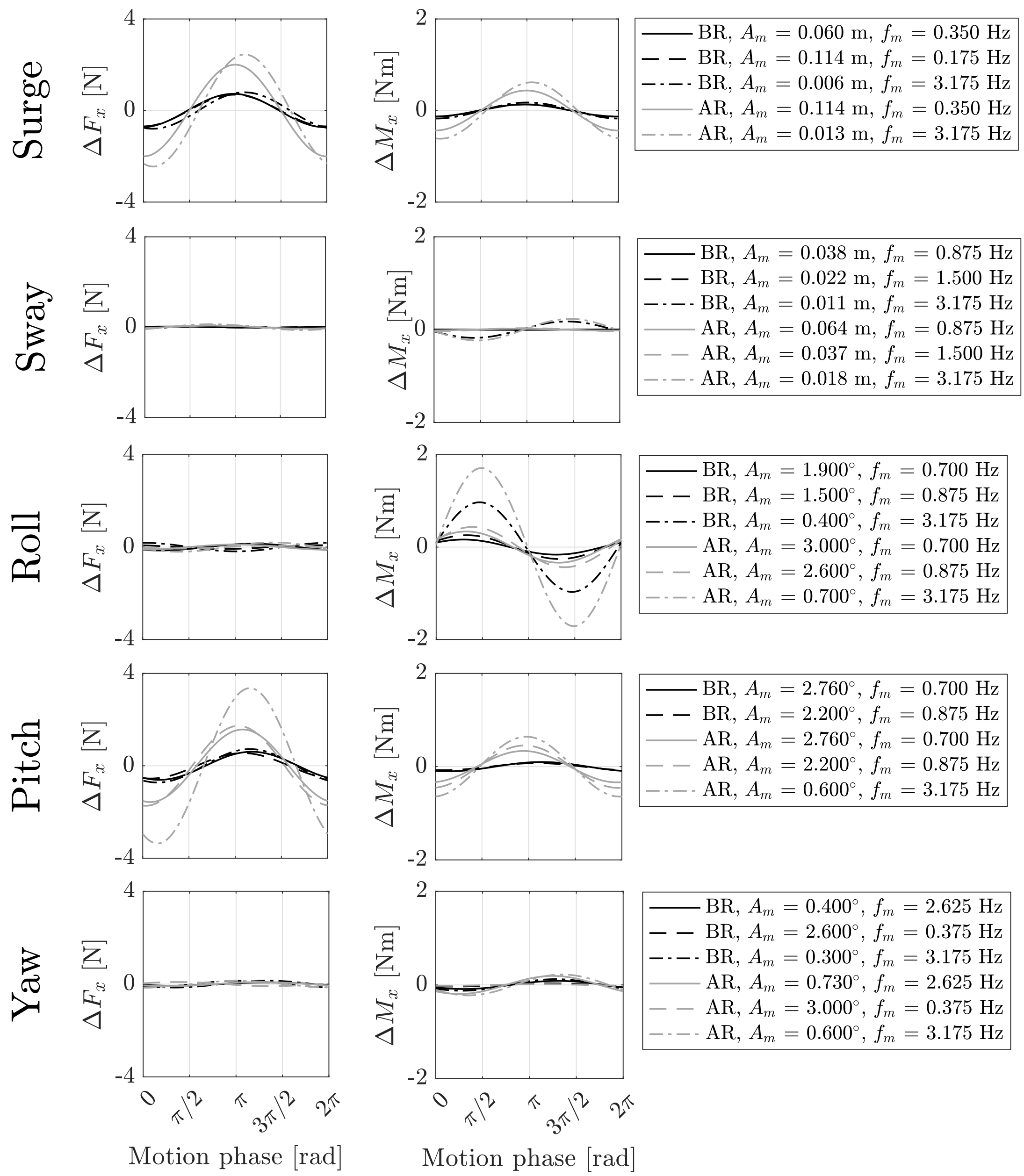

Figure 5. Harmonic component of dynamic thrust (ΔF_x) and dynamic torque (ΔM_x) at the frequency of motion in one period for different type of platform motion. BR is below rated, AR is above rated.

where ρ is the air density, C_T the thrust coefficient A_r the rotor area, and U the wind speed; and the aerodynamic torque as

$$M_x = \frac{1}{2}\rho C_Q(\omega_r, \beta, U) A_r \mathrm{R} U^2 \,, \tag{5}$$

https://doi.org/10.5194/wes-2022-36
Preprint. Discussion started: 8 April 2022

where C_Q is the torque coefficient, and R is the rotor radius. The first-order linearization of Eq. 4 and Eq. 5 is

$$F_x \simeq F_{x,0} + \left.\frac{\partial F_x}{\partial \omega_r}\right|_0 (\omega_r - \omega_{r,0}) + \left.\frac{\partial F_x}{\partial \beta}\right|_0 (\beta - \beta_0) + \left.\frac{\partial F_x}{\partial u}\right|_0 (u - U_0)\,, \tag{6}$$

$$M_x \simeq M_{x,0} + \left.\frac{\partial M_x}{\partial \omega_r}\right|_0 (\omega_r - \omega_{r,0}) + \left.\frac{\partial M_x}{\partial \beta}\right|_0 (\beta - \beta_0) + \left.\frac{\partial M_x}{\partial u}\right|_0 (u - U_0)\,, \tag{7}$$

where $(\cdot)_0$ denotes the steady-state value of a quantity for a given turbine operating point. In these experiments, the blade pitch and rotor speed were constant, and the apparent wind speed for the rotor changed due to platform surge and pitch motion. In this case Eq. 6 and Eq. 7 become

$$F_x \simeq F_{x,0} - \dot{x}_{\mathrm{hub}} \left.\frac{\partial F_x}{\partial U}\right|_0\,, \tag{8}$$

$$M_x \simeq M_{x,0} - \dot{x}_{\mathrm{hub}} \left.\frac{\partial M_x}{\partial U}\right|_0\,, \tag{9}$$

where $\dot{x}_{\mathrm{hub}}$ is the hub velocity. With harmonic motion, the variation of thrust force and torque with respect to the steady-state value is

$$\Delta F_x(t) = -K_{u,T}(2\pi f_m) A_{\mathrm{hub}} \sin(2\pi f_m t - \pi/2)\,, \tag{10}$$

$$\Delta M_x(t) = -K_{u,Q}(2\pi f_m) A_{\mathrm{hub}} \sin(2\pi f_m t - \pi/2)\,, \tag{11}$$

with $K_{u,T} = \partial F_x/\partial U|_0$, $K_{u,Q} = \partial M_x/\partial U|_0$, and $A_{\mathrm{hub}} = A_m$ in case of surge motion, and $A_{\mathrm{hub}} = A_m h_{\mathrm{hub}}$ for pitch motion. The phase of the force response with respect to motion is $-\pi/2$. The zero-peak amplitude normalized by amplitude of hub motion is

$$\overline{\Delta F_x}/A_{\mathrm{hub}} = K_{u,T}(2\pi f_m)\,, \tag{12}$$

$$\overline{\Delta M_x}/A_{\mathrm{hub}} = K_{u,Q}(2\pi f_m)\,, \tag{13}$$

so it is proportional to the frequency of motion by the slope of the steady thrust/torque coefficient evaluated at the steady-state operating point. This approach is referred to as quasi-steady theory (QST) because it predicts the aerodynamic response in dynamic wind conditions caused by platform motion based on the aerodynamic response at steady state (i.e., the C_T and C_P maps of Fig. 3). This linearized aerodynamic model is widely used in floating turbine control. One example is the paper of van der Veen et al. (2012) uses this approach to explain the negative-damping phenomenon associated with pitch control

https://doi.org/10.5194/wes-2022-36
Preprint. Discussion started: 8 April 2022

in above rated wind for floating turbines. Abbas et al. (2022) used it to introduce an additional feedback term in the pitch controller in order to decouple the platform pitch and the rotor dynamics and stabilize the system. The quasi-steady approach is used in its nonlinear form of Eq. 4-5 in the low-order floating turbine model of Lemmer et al. (2020a). After linearization, the model is used by Lemmer et al. (2020b) to define a gain scheduling function for the turbine pitch controller aimed at stabilizing the response of the system.

Figure 6 compares the thrust and torque response to surge and pitch motion from the experiment and from the QST model of Eq. 12-13, obtained as

$$K_{u,T} = \left.\frac{\partial F_x}{\partial U}\right|_0 = \frac{F_{x,0}}{\omega_{\mathrm{r},0}}\left(2 - \left.\frac{\partial C_T}{\partial \lambda}\right|_0 \frac{\lambda_0}{C_{t,0}}\right), \tag{14}$$

$$K_{u,Q} = \left.\frac{\partial M_x}{\partial U}\right|_0 = \frac{M_{x,0}}{\omega_{\mathrm{r},0}}\left(2 - \left.\frac{\partial C_Q}{\partial \lambda}\right|_0 \frac{\lambda_0}{C_{q,0}}\right), \tag{15}$$

where λ is the TSR. The slope depends solely on the turbine operating condition and the consequent steady-state response, so Eq. 14-15 are evaluated for both the operating conditions of the experiment: $F_{x,0}$ and $M_{x,0}$ are those of fixed-turbine tests (see Table 3), the partial derivatives of the rotor coefficients are obtained from the gradient of the rotor coefficients map shown in Fig. 3, with $C_Q = C_P/\lambda$. The C_T and C_Q coefficients were measured for TSR increments of 0.3, which is similar to the variation of TSR caused by surge and pitch motion in the load cases of the experiment (0.16-0.29), and with pitch increments of 3°. In Fig 6 we see the response to surge motion is quasi-static except than at 3.175 Hz. Below this frequency the response amplitude is linear with frequency and the phase-shift with respect to motion is $-\pi/2$; the amplitude is close to the QST prediction and the agreement is better in below-rated wind. The difference in slope between the linear fit and the QST in above-rated wind can be due to the interpolation of $\partial C_T \partial\lambda|_0$ and $\partial C_Q \partial\lambda|_0$ which is required to evaluate the derivatives for the a pitch angle of $8.5°$. The good agreement with QST in case of surge motion is in agreement with the findings of Fontanella et al. (2021a) where the same result was obtained for low-frequency motion of a 1:75 scale model of the DTU 10 MW. The point at 3.175 Hz shows a response amplitude higher than the linear trend, and the phase shift is lower than $-\pi/2$. QST is not predictive for this condition: a large part of the blade is likely interested by blade-level unsteady aerodynamics for a motion frequency of 3.175 Hz ("Wave" in Fig. 2) and this explains the non-quasi-static response to this condition of motion. Also in the case of pitch motion, the amplitude of torque and thrust is linear with frequency except for the point at 3.175 Hz, which shows a higher response amplitude than what is predicted by QST. In case of pitch, the phase is not $-\pi/2$ for any frequency. To sum up, experimental data show the QST model is valid for the thrust/torque response to low-frequency surge motion. Instead, we observe some differences for higher-frequency motion, as it occurs as a consequence of wave excitation, and pitch motion.

5 Results about wake

This section describes results about hot-wire measurements. Focus of the analysis is the effect of platform motion at wave-peak frequency (f_m = 3.175 Hz) on the axial velocity. This is examined because, in a wind farm perspective, it defines the inflow conditions for downstream turbines.

https://doi.org/10.5194/wes-2022-36
Preprint. Discussion started: 8 April 2022

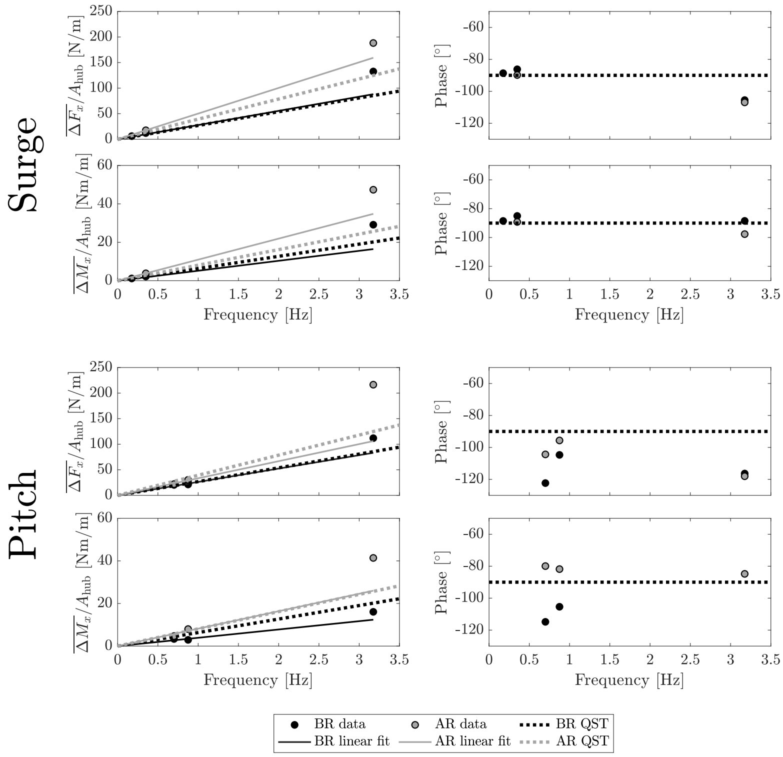

Figure 6. The thrust and torque responses to surge and pitch motion in below rated (BR) and above rated (AR) wind is compared to quasi-steady theory (QST) in terms of normalized zero-peak amplitude and phase shift with respect to platform motion. The linear fit is the least-square linear regression of amplitude data which is obtained excluding the point at 3.175 Hz and intercepts the axes in the origin; QST is the prediction of the quasi-steady theory model computed from the steady-state thrust and torque coefficient maps of Fig. 3.

Figure 7 shows the average wake deficit normalized by the free-stream velocity U_∞ at $\mathrm{X} = 2.3\mathrm{D}$ for different types of motion. The wake shape is defined by the turbine operating condition, and shows a double-gaussian profile in below rated wind cases, and a gaussian profile in above rated-cases. In both conditions the wake shape is not symmetric with respect to the rotor axis, and velocity is generally lower for negative-Y. This behavior was also seen in the wake measurements of Fontanella et al. (2021a), which were with a different rotor but in the same wind tunnel, and this supports the idea it is due to the wind tunnel characteristics more than the wind turbine model or the experimental setup. In particular, it can be caused by anisotropic blockage, which hinders the wake expansion on one side more than the other. The velocity at the wake extremities is about 15% higher than the free-stream velocity, and this is a consequence of blockage.

The wake with motion is compared to the fixed turbine case computing the average wake deficit for the rotor area, defined as:

$$D_{\mathrm{avg}} = \frac{1}{U_\infty}\left(\frac{\sum_{i=1}^{N}|y_i|U_i}{\sum_{i=1}^{N}|y_i|}\right), \tag{16}$$

https://doi.org/10.5194/wes-2022-36
Preprint. Discussion started: 8 April 2022

with $y_i = -1.2, \ldots, 1.2$, and $N = 25$. The results are reported in Table 4 and show that the average velocity across the rotor is slightly lower with motion compared to the fixed case. In a wind farm perspective, this means the energy in the flow available for a hypothetical floating turbine at 2.3D distance from the upstream unit working in fully-waked condition would be slightly less than in the bottom-fixed case. The bottom panels of Fig. 7 show the wake deficit increment with motion compared to the bottom-fixed case for different Y positions. This information might be used to compute the change in the radial distribution of aerodynamic loads for a waked floating turbine. In below rated wind, the velocity is lower in correspondence of the outer sections of the rotor, and increased outside it; the variation is about the same regardless of the type of motion. In above rated wind, the velocity is decreased between $\mathrm{Y} = \pm(0.5\text{-}1)$ m, and the largest decrement is with sway, pitch, and yaw motion. Sway has the lowest difference for below rated but the highest difference for the above rated.

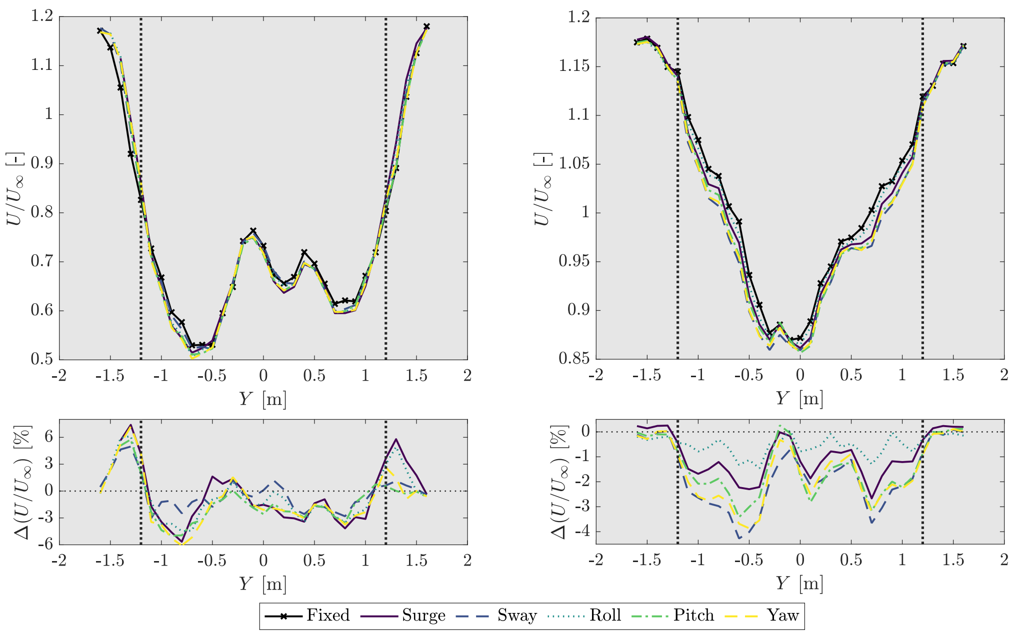

Figure 7. Average wake deficit at $\mathrm{X} = 2.3\mathrm{D}$ for the fixed case and with different motions, in below rated (top left) and above rated (top right) wind. $\Delta(U/U_\infty)$ is the wake deficit increment with motion with respect to the fixed case (below rated: bottom left; above rated: bottom right). The vertical dotted lines mark the edge of the rotor.

Ramos-García et al. (2021) and Fu et al. (2019) observed the wake recovery for a pitching turbine is different than in the bottom-fixed case: flow mixing is higher for a floating turbine because increased turbulence due to motion helps promoting a faster break down of the strong vortex structures. In this sense, Fig. 8 complements Fig. 7 by showing the turbulence kinetic energy (i.e., $k = \frac{1}{2}(\sigma_u^2 + \sigma_v^2 + \sigma_w^2)$, where σ_i is the variance of the i-th velocity component) at $\mathrm{X} = 2.3\mathrm{D}$ for the fixed turbine and with different types of platform motion at the wave peak frequency. The distribution of k about the Y axis is given by the turbine operating condition and is consistent for the fixed and floating scenario. In below rated wind, most of the turbulence kinetic energy is concentrated around the edge of the rotor, and is associated with tip vortices. In above rated, k is maximum

https://doi.org/10.5194/wes-2022-36
Preprint. Discussion started: 8 April 2022

Table 4. Average wake deficit for the rotor area for the two wind conditions (below rated BR, above rated AR) and different motions at the wave frequency (f_m = 3.175 Hz). Δ is the percent change with motion with respect to the fixed case.

Condition	BR	ΔBR	AR	ΔAR
	[-]	[%]	[-]	[%]
Fixed	0.667	-	1.034	-
Surge	0.660	-1.079	1.021	-1.300
Sway	0.661	-0.884	1.011	-2.310
Roll	0.659	-1.319	1.028	-0.609
Pitch	0.657	-1.604	1.015	-1.876
Yaw	0.657	-1.589	1.013	-2.117

between $\mathrm{Y} = -0.5\text{-}0\ \mathrm{m}$, which corresponds to the wake center, and the peak is likely associated with root vortices. k is non-symmetric, and is more pronounced at negative-Y. With motion, k is generally lower than for the bottom-fixed case, except at the rotor edge for the above-rated case. The high-frequency platform oscillations caused by response to wave forcing seems to produce a stronger and more stable wake. The lower flow mixing makes the wake recover more slowly than without motion. This agrees with what was observed by Ramos-García et al. (2021) for pitch motion at 0.057 Hz (i.e.,1.622 Hz at model scale). The authors noticed that for lower motion frequencies differences between a bottom-fixed and floating turbine are significant for $x/\mathrm{D} > 5$, but for higher frequencies the wake recovery is independent of the downstream location.

Velocity fluctuations are expected to happen for different reasons with different types of motion. With surge and pitch, these occur due to the dynamic inflow created by the motion and the oscillating thrust force. Considering the motion in the other directions, the magnitude of the wind speed perceived by the rotor is similar to the fixed case, and oscillations of the axial velocity in the wake are explained as the effect of wake meandering: the velocity at a downstream location varies periodically because the wake is moved laterally and vertically. This occurs also with pitch and is superposed to the effect of dynamic inflow. The presence and relevance of velocity oscillations in the wake due to motion is assessed from the phase-averaged time series obtained by averaging data of 94 motion cycles. This way of processing data keeps the signal content which has the same periodicity of motion, filtering out the rest. The phase-averaged time series of the axial velocity u at $\mathrm{X} = 2.3\mathrm{D}$ and at $\mathrm{Y} = 0\mathrm{R}$ (center of the wake) is shown in Fig. 9. The figure also shows the harmonic component of u at the frequency of motion. In below rated wind the amplitude of velocity fluctuations associated with motion is small, less 1% of U_∞, and similar in magnitude to the turbulence in the wake of the fixed turbine. In above rated wind the harmonic at the frequency of motion is clearly present with sway, roll and pitch. Sway and roll move the wake along the Y-Z plane and pitch moves the wake in X-Z plane. This may explain the periodically-varying axial velocity. In contrast, it seems that yaw does not move the wake center in a significant way. In wind farm control studies a static yaw is often used for redirecting the wake laterally (Meyers et al. (2022)), however oscillating yaw does not seem an effective way of disturbing the wake direction. The tracking methods for the wake center described by Coudou et al. (2018) was applied to measurements with sway and roll, and the wake center

https://doi.org/10.5194/wes-2022-36
Preprint. Discussion started: 8 April 2022

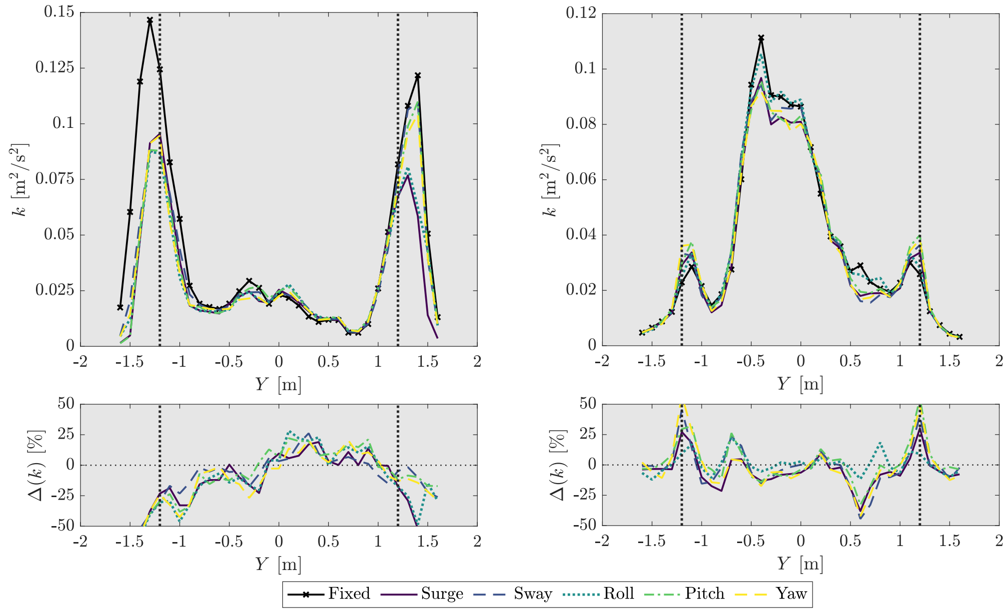

Figure 8. Turbulence kinetic energy at X = 2.3D for the fixed case and with different motions, in below rated (left) and above rated (right) wind. $\Delta(k)$ is the turbulence kinetic energy increment with motion with respect to the fixed case (below rated: bottom left; above rated: bottom right). The vertical dotted lines mark the edge of the rotor.

position obtained from the algorithm results constant in time. If the wake core moves, the motion is smaller than the spatial resolution of wake data (i.e., 100 mm, or 10 m full-scale).

6 Conclusions

Wind tunnel testing has been conducted to characterize the aerodynamic response of a 1:100 scale model of the IEA 15 MW subjected to harmonic platform motion. The turbine is forced moving in five motion directions; for every type of motion we considered different combinations of amplitude and frequency, selected to be representative of the dynamic response of the two 15 MW floating turbines of the COREWIND project.

The rotor response to platform motion is examined with focus on rotor-integral loads, thrust and torque. Surge and pitch motion move the turbine rotor in the wind direction altering the apparent wind speed. As a consequence, thrust and torque show large-amplitude oscillations. The main effect of motion in the other directions (i.e., sway, roll, and yaw) is to introduce wind shear and to alter the direction of the wind perceived by rotor, whereas the impact on relative wind speed is limited. The aerodynamic response to these motion is small. The aerodynamic thrust and torque are often introduced in control-oriented models as rotor-integral loads defined by means of the static thrust and torque coefficients or, when the model is linearized, with the derivatives of static coefficients with respect to rotor speed, wind speed, and pitch angle. Here we examined the response

https://doi.org/10.5194/wes-2022-36
Preprint. Discussion started: 8 April 2022

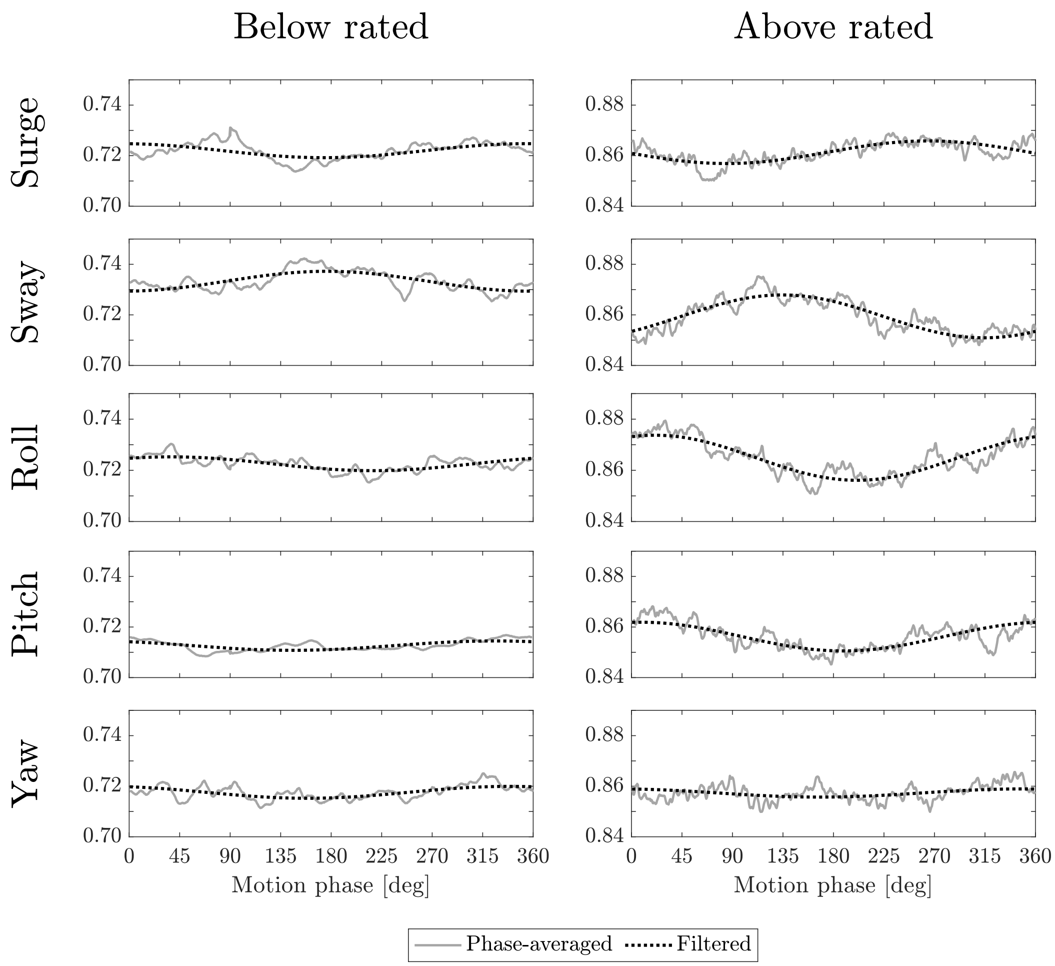

Figure 9. Time series of the axial velocity normalized by the free-stream wind speed u/U_∞ in one motion cycle at $\mathrm{X} = 2.3\mathrm{D}$ and $\mathrm{Y} = 0\mathrm{R}$ with different motions and in two wind conditions. Phase-averaged data of 94 motion cycles are compared to the harmonic of the signal at the frequency of motion ("Filtered").

of such quasi-static aerodynamic model to the harmonic oscillation of wind speed created by surge and pitch motion. The turbine loads measured in the experiments with surge motion are aligned to the model predictions, except for motion at wave frequency. Here, blade-level unsteady aerodynamics may occur, which is not accounted for by the quasi-static model. The model predictions are instead good for low-frequency motion. In case of pitch, the amplitude of thrust and torque oscillations with low-frequency motion is predicted with reasonable accuracy by the quasi-static model, but the phase is not. The difference in phase shift can be due to the inflow conditions created pitch motion which is non-uniform across the rotor, or by other phenomena not considered in this analysis. Also with pitch, the quasi-static model is not predictive for wave-frequency motion.

https://doi.org/10.5194/wes-2022-36
Preprint. Discussion started: 8 April 2022

The analysis of the aerodynamics-load response led to the following conclusions. The fact that the aerodynamic thrust and torque are largely influenced by surge and pitch motion, supports the idea of including these two degrees-of-freedom in coupled models of floating turbines. Reduced-order models which focus is the global dynamics of the system may instead neglect motion in the other directions. Quasi-static aerodynamic models are predictive for low-frequency surge motion. The QST model is sensitive to the accuracy of the static coefficients from which it is derived. Discrepancies are seen in case of wave-frequency motion and pitch motion in general. Since the turbine response in the pitch direction is largely influenced by aerodynamic thrust force, and this is also the root cause of control issues in floating turbines, it is advised that future experimental efforts should focus on pitch motion.

Wind speed in the turbine wake was measured at hub-height, 2.3D downwind the rotor, for the fixed turbine and imposing platform motion in five directions; the motion frequency was equal to the wave frequency at the Gran Canaria site (Mahfouz et al. (2021)). The experiment shows that the average axial-velocity in the wake in correspondence of the rotor disk is slightly lower with motion compared to the fixed case. In the motion conditions at hand, the wake recovery appears to be slower than for a bottom-fixed turbine. The turbulence kinetic energy in the wake is generally lower with motion than for a bottom-fixed turbine, hence the wake is more stable. The lower flow mixing may explain the lower wake recovery. Axial velocity in the wake of the floating turbine has oscillations at the same frequency of the imposed motion. These are due to the dynamic inflow created by motion and the effect of wake meandering. The additional oscillations in the wake velocity should be taken into account in studies about floating farms, because they represent an additional forcing for waked turbines. In above rated wind, dynamic motion of the wake center occurs with sway, roll and pitch; in contrast, oscillating yaw does not seem to be very effective for perturbing the wake position. This rises questions about if and how dynamic platform motion can be controlled and exploited for wake control. Concerning the wake of floating turbines, suggestion for future work is to measure the wake further downstream. Here, we considered a non-turbulent inflow condition to highlight the effects of platform motion, but measurement with turbulence are advisable to understand the effect of inflow turbulence on wake mixing.

Data availability. The dataset is accessible upon request to the authors.

https://doi.org/10.5194/wes-2022-36
Preprint. Discussion started: 8 April 2022

Appendix A: Test matrices

Table A1. Test matrix for cases with motion. f_m is the frequency of motion, A_m the amplitude, TSR is the tip-speed ratio and CP the collective pitch. Wake measurements were carried out for load cases where a × is present in the "Wake" column.

Type	Wind speed [m/s]	f_m [Hz]	A_m [m | °]	Rotor speed [rpm]	TSR [-]	CP [°]	Wake
Surge	3.0	0.350	0.060	210	8.8	-3.0	
Surge	3.0	0.175	0.114	210	8.8	-3.0	
Surge	3.0	3.175	0.006	210	8.8	-3.0	×
Surge	5.0	0.350	0.114	216	5.4	8.5	
Surge	5.0	0.175	0.180	216	5.4	8.5	
Surge	5.0	3.175	0.013	216	5.4	8.5	×
Sway	3.0	0.875	0.038	210	8.8	-3.0	
Sway	3.0	1.500	0.022	210	8.8	-3.0	
Sway	3.0	3.175	0.011	210	8.8	-3.0	×
Sway	5.0	0.875	0.064	216	5.4	8.5	
Sway	5.0	1.500	0.037	216	5.4	8.5	
Sway	5.0	3.175	0.018	216	5.4	8.5	×
Roll	3.0	0.700	1.900	210	8.8	-3.0	
Roll	3.0	0.875	1.500	210	8.8	-3.0	
Roll	3.0	3.175	0.400	210	8.8	-3.0	×
Roll	5.0	0.700	3.000	216	5.4	8.5	
Roll	5.0	0.875	2.600	216	5.4	8.5	
Roll	5.0	3.175	0.700	216	5.4	8.5	×
Pitch	3.0	0.700	1.150	210	8.8	-3.0	
Pitch	3.0	0.875	1.000	210	8.8	-3.0	
Pitch	3.0	3.175	0.250	210	8.8	-3.0	×
Pitch	5.0	0.700	2.760	216	5.4	8.5	
Pitch	5.0	0.875	2.200	216	5.4	8.5	
Pitch	5.0	3.175	0.600	216	5.4	8.5	×
Yaw	3.0	2.625	0.400	210	8.8	-3.0	
Yaw	3.0	0.375	2.600	210	8.8	-3.0	
Yaw	3.0	3.175	0.300	210	8.8	-3.0	×
Yaw	5.0	2.625	0.730	216	5.4	8.5	
Yaw	5.0	0.375	3.000	216	5.4	8.5	
Yaw	5.0	3.175	0.600	216	5.4	8.5	×

Author contributions. AFo and AFa designed the wind tunnel experiments, which were carried out with the help of SDC. Data were processed by AFo. MB and AFa supervised the work and the project in a larger perspective. All coauthors thoroughly reviewed the article.

415 *Competing interests.* The authors declare that they have no conflict of interest.

Acknowledgements. This research, including the open-access publication, has been supported by Horizon 2020 project COREWIND (grant no. 815083).

References

Abbas, N. J., Zalkind, D. S., Pao, L., and Wright, A.: A reference open-source controller for fixed and floating offshore wind turbines, Wind Energy Science, 7, 53–73, https://doi.org/10.5194/wes-7-53-2022, https://wes.copernicus.org/articles/7/53/2022/, 2022.

Allen, C., Viselli, A., Dagher, H., Goupee, A., Gaertner, E., Abbas, N., Hall, M., and Barter, G.: Definition of the UMaine VolturnUS-S Reference Platform Developed for the IEA Wind 15-Megawatt Offshore Reference Wind Turbine, Tech. rep., National Renewable Energy Laboratory, https://www.nrel.gov/docs/fy20osti/76773.pdf, Available at https://www. nrel.gov/docs/fy20osti/76773.pdf, 2020.

Barter, G. E., Robertson, A., and Musial, W.: A systems engineering vision for floating offshore wind cost optimization, Renewable Energy Focus, 34, 1–16, https://doi.org/https://doi.org/10.1016/j.ref.2020.03.002, https://www.sciencedirect.com/science/article/pii/S1755008420300132, 2020.

Battistella, T., Paradinas, D. D. L. D., Urban, A. M., and Garcia, R. G.: High Fidelity Simulation of Multi-MW Rotor Aerodynamics by Using a Multifan, vol. Volume 10: Ocean Renewable Energy of *International Conference on Offshore Mechanics and Arctic Engineering*, https://doi.org/10.1115/OMAE2018-77606, https://doi.org/10.1115/OMAE2018-77606, v010T09A074, 2018.

Bayati, I., Belloli, M., Bernini, L., and Zasso, A.: Wind tunnel validation of AeroDyn within LIFES50+ project: imposed Surge and Pitch tests, Journal of Physics: Conference Series, 753, 092 001, https://doi.org/10.1088/1742-6596/753/9/092001, https://doi.org/10.1088/1742-6596/753/9/092001, 2016.

Bayati, I., Belloli, M., Bernini, L., and Zasso, A.: Aerodynamic design methodology for wind tunnel tests of wind turbine rotors, Journal of Wind Engineering and Industrial Aerodynamics, 167, 217 – 227, https://doi.org/https://doi.org/10.1016/j.jweia.2017.05.004, http://www.sciencedirect.com/science/article/pii/S0167610517301368, 2017a.

Bayati, I., Belloli, M., Bernini, L., and Zasso, A.: Wind Tunnel Wake Measurements of Floating Offshore Wind Turbines, vol. 137, pp. 214–222, https://doi.org/10.1016/j.egypro.2017.10.375, https://www.scopus.com/inward/record.uri?eid=2-s2.0-85032015856&doi=10.1016%2fj.egypro.2017.10.375&partnerID=40&md5=aac148722a514dec153f833fee76b361, 2017b.

Bayati, I., Belloli, M., Bernini, L., Boldrin, D., Boorsma, K., Caboni, M., Cormier, M., Mikkelsen, R., Lutz, T., and Zasso, A.: UNAFLOW project: UNsteady Aerodynamics of FLOating Wind turbines, Journal of Physics: Conference Series, 1037, 072 037, https://doi.org/10.1088/1742-6596/1037/7/072037, https://doi.org/10.1088/1742-6596/1037/7/072037, 2018a.

Bayati, I., Bernini, L., Zanotti, A., Belloli, M., and Zasso, A.: Experimental investigation of the unsteady aerodynamics of FOWT through PIV and hot-wire wake measurements, Journal of Physics: Conference Series, 1037, 052 024, https://doi.org/10.1088/1742-6596/1037/5/052024, https://doi.org/10.1088/1742-6596/1037/5/052024, 2018b.

Belloli, M., Bayati, I., Facchinetti, A., Fontanella, A., Giberti, H., La Mura, F., Taruffi, F., and Zasso, A.: A hybrid methodology for wind tunnel testing of floating offshore wind turbines, Ocean Engineering, 210, https://doi.org/10.1016/j.oceaneng.2020.107592, https://www.scopus.com/inward/record.uri?eid=2-s2.0-85085751799&doi=10.1016%2fj.oceaneng.2020.107592&partnerID=40&md5=e3b5533c595a58bc2d7e7684dc63bb95, 2020.

Cormier, M., Caboni, M., Lutz, T., Boorsma, K., and Kramer, E.: Numerical analysis of unsteady aerodynamics of floating offshore wind turbines, Journal of Physics: Conference Series, 1037, 072 048, https://doi.org/10.1088/1742-6596/1037/7/072048, https://doi.org/10.1088%2F1742-6596%2F1037%2F7%2F072048, 2018.

Coudou, N., Moens, M., Marichal, Y., Beeck, J. V., Bricteux, L., and Chatelain, P.: Development of wake meandering detection algorithms and their application to large eddy simulations of an isolated wind turbine and a wind farm, Journal of Physics: Conference Series, 1037, 072 024, https://doi.org/10.1088/1742-6596/1037/7/072024, https://doi.org/10.1088/1742-6596/1037/7/072024, 2018.

Farrugia, R., Sant, T., and Micallef, D.: Investigating the aerodynamic performance of a model offshore floating wind turbine, Renewable Energy, 70, 24–30, https://doi.org/https://doi.org/10.1016/j.renene.2013.12.043, https://www.sciencedirect.com/science/article/pii/S0960148114000147, special issue on aerodynamics of offshore wind energy systems and wakes, 2014.

Ferreira, C., Yu, W., Sala, A., and Vire, A.: Dynamic inflow model for a Floating Horizontal Axis Wind Turbine in surge motion, Wind Energy Science Discussions, 2021, 1–22, https://doi.org/10.5194/wes-2021-34, https://wes.copernicus.org/preprints/wes-2021-34/, 2021.

Fontanella, A., Al, M., van der Hoek, D., Liu, Y., van Wingerden, J., and Belloli, M.: A control-oriented wave-excited linear model for offshore floating wind turbines, Journal of Physics: Conference Series, 1618, 022 038, https://doi.org/10.1088/1742-6596/1618/2/022038, https://doi.org/10.1088/1742-6596/1618/2/022038, 2020.

Fontanella, A., Bayati, I., Mikkelsen, R., Belloli, M., and Zasso, A.: UNAFLOW: a holistic wind tunnel experiment about the aerodynamic response of floating wind turbines under imposed surge motion, Wind Energy Science, 6, 1169–1190, https://doi.org/10.5194/wes-6-1169-2021, https://wes.copernicus.org/articles/6/1169/2021/, 2021a.

Fontanella, A., Bayati, I., Mikkelsen, R., Belloli, M., and Zasso, A.: UNAFLOW: UNsteady Aerodynamics of FLOating Wind turbines, https://doi.org/10.5281/zenodo.4740006, https://doi.org/10.5281/zenodo.4740006, https://doi.org/10.5281/zenodo.4740006, 2021b.

Fu, S., Jin, Y., Zheng, Y., and Chamorro, L. P.: Wake and power fluctuations of a model wind turbine subjected to pitch and roll oscillations, Applied Energy, 253, 113 605, https://doi.org/https://doi.org/10.1016/j.apenergy.2019.113605, https://www.sciencedirect.com/science/article/pii/S0306261919312796, 2019.

Lemmer, F., Yu, W., Luhmann, B., Schlipf, D., and Cheng, P. W.: Multibody modeling for concept-level floating offshore wind turbine design, Multibody System Dynamics, 49, 203 – 236, https://doi.org/10.1007/s11044-020-09729-x, https://doi.org/10.1007/s11044-020-09729-x, 2020a.

Lemmer, F., Yu, W., Schlipf, D., and Cheng, P. W.: Robust gain scheduling baseline controller for floating offshore wind turbines, Wind Energy, 23, 17–30, https://doi.org/10.1002/we.2408, https://onlinelibrary.wiley.com/doi/abs/10.1002/we.2408, 2020b.

Mahfouz, M. Y., Molins, C., Trubat, P., Hernández, S., Vigara, F., Pegalajar-Jurado, A., Bredmose, H., and Salari, M.: Response of the International Energy Agency (IEA) Wind 15 MW WindCrete and Activefloat floating wind turbines to wind and second-order waves, Wind Energy Science, 6, https://doi.org/10.5194/wes-6-867-2021, https://wes.copernicus.org/articles/6/867/2021/, 2021.

Mancini, S., Boorsma, K., Caboni, M., Cormier, M., Lutz, T., Schito, P., and Zasso, A.: Characterization of the unsteady aerodynamic response of a floating offshore wind turbine, https://doi.org/10.5194/wes-2020-94, 2020.

Meyers, J., Bottasso, C., Dykes, K., Fleming, P., Gebraad, P., Giebel, G., Göçmen, T., and van Wingerden, J.-W.: Wind farm flow control: prospects and challenges, Wind Energy Science Discussions, 2022, 1–56, https://doi.org/10.5194/wes-2022-24, https://wes.copernicus.org/preprints/wes-2022-24/, 2022.

Nanos, E. M., Bottasso, C. L., Manolas, D. I., and Riziotis, V. A.: Vertical wake deflection for floating wind turbines by differential ballast control, Wind Energy Science Discussions, 2021, 1–30, https://doi.org/10.5194/wes-2021-79, https://wes.copernicus.org/preprints/wes-2021-79/, 2021.

Pegalajar-Jurado, A., Borg, M., and Bredmose, H.: An efficient frequency-domain model for quick load analysis of floating offshore wind turbines, Wind Energy Science, 3, 693–712, https://doi.org/10.5194/wes-3-693-2018, https://wes.copernicus.org/articles/3/693/2018/, 2018.

Ramos-García, N., Kontos, S., Pegalajar-Jurado, A., González Horcas, S., and Bredmose, H.: Investigation of the floating IEA Wind 15 MW RWT using vortex methods Part I: Flow regimes and wake recovery, Wind Energy, pp. 1–37, https://doi.org/https://doi.org/10.1002/we.2682, https://onlinelibrary.wiley.com/doi/abs/10.1002/we.2682, 2021.

https://doi.org/10.5194/wes-2022-36
Preprint. Discussion started: 8 April 2022

Rockel, S., Camp, E., Schmidt, J., Peinke, J., Cal, R. B., and Hölling, M.: Experimental Study on Influence of Pitch Motion on the Wake of a Floating Wind Turbine Model, Energies, 7, 1954–1985, https://doi.org/10.3390/en7041954, https://www.mdpi.com/1996-1073/7/4/1954, 2014.

Schliffke, B., Aubrun, S., and Conan, B.: Wind Tunnel Study of a "Floating" Wind Turbine's Wake in an Atmospheric Boundary Layer with Imposed Characteristic Surge Motion, Journal of Physics: Conference Series, 1618, 062 015, https://doi.org/10.1088/1742-6596/1618/6/062015, https://doi.org/10.1088/1742-6596/1618/6/062015, 2020.

Sebastian, T. and Lackner, M.: Characterization of the unsteady aerodynamics of offshore floating wind turbines, Wind Energy, 16, 339–352, https://doi.org/https://doi.org/10.1002/we.545, https://onlinelibrary.wiley.com/doi/abs/10.1002/we.545, 2013.

Stoelzle, M. and Stein, L.: Rainbow color map distorts and misleads research in hydrology – guidance for better visualizations and science communication, Hydrology and Earth System Sciences, 25, 4549–4565, https://doi.org/10.5194/hess-25-4549-2021, https://hess.copernicus.org/articles/25/4549/2021/, 2021.

van der Veen, G., Couchman, I., and Bowyer, R.: Control of floating wind turbines, in: 2012 American Control Conference (ACC), pp. 3148–3153, https://doi.org/10.1109/ACC.2012.6315120, 2012.

Veers, P., Dykes, K., Lantz, E., Barth, S., Bottasso, C. L., Carlson, O., Clifton, A., Green, J., Green, P., Holttinen, H., Laird, D., Lehtomäki, V., Lundquist, J. K., Manwell, J., Marquis, M., Meneveau, C., Moriarty, P., Munduate, X., Muskulus, M., Naughton, J., Pao, L., Paquette, J., Peinke, J., Robertson, A., Rodrigo, J. S., Sempreviva, A. M., Smith, J. C., Tuohy, A., and Wiser, R.: Grand challenges in the science of wind energy, Science, 366, eaau2027, https://doi.org/10.1126/science.aau2027, https://www.science.org/doi/abs/10.1126/science.aau2027, 2019.

Wang, C., Campagnolo, F., Canet, H., Barreiro, D. J., and Bottasso, C. L.: How realistic are the wakes of scaled wind turbine models?, Wind Energy Science, 6, 961–981, https://doi.org/10.5194/wes-6-961-2021, https://wes.copernicus.org/articles/6/961/2021/, 2021.

Wise, A. S. and Bachynski, E. E.: Wake meandering effects on floating wind turbines, Wind Energy, 23, 1266–1285, https://doi.org/10.1002/we.2485, https://onlinelibrary.wiley.com/doi/abs/10.1002/we.2485, 2020.